

RESEARCH ARTICLE

10.1002/2015JA022253

Key Points:

- TEC responds to Pc4 “giant pulsations (Pgs)”
- TEC and magnetic field exhibit similar quasi-sinusoidal, highly regular waveforms
- Multisatellite observations indicate that the TEC response was intermittent and localized

Correspondence to:

C. Watson,
chris.watson@unb.ca

Citation:

Watson, C., P. T. Jayachandran, H. J. Singer, R. J. Redmon, and D. Danskin (2016), GPS TEC response to Pc4 “giant pulsations”, *J. Geophys. Res. Space Physics*, 121, 1722–1735, doi:10.1002/2015JA022253.

Received 8 DEC 2015

Accepted 25 JAN 2016

Accepted article online 28 JAN 2016

Published online 23 FEB 2016

GPS TEC response to Pc4 “giant pulsations”

Chris Watson¹, P. T. Jayachandran¹, Howard J. Singer², Robert J. Redmon³, and Donald Danskin⁴

¹Physics Department, University of New Brunswick, Fredericton, New Brunswick, Canada, ²NOAA Space Weather Prediction Center, Boulder, Colorado, USA, ³NOAA National Centers for Environmental Information, Boulder, Colorado, USA, ⁴Natural Resources Canada, Ottawa, Ontario, Canada

Abstract Variations in ionospheric total electron content (TEC) associated with ultralow frequency (ULF) magnetic field variations in the Pc4 (6.7–22.0 MHz) frequency band were observed in the early morning sector. TEC variations were observed by the Global Positioning System (GPS) receiver in Sanikiluaq, Nunavut (56.54°N, 280.77°E), which is located near the equatorward edge of the auroral region. Small-amplitude Pc4 ULF waves were observed by the Sanikiluaq ground magnetometer and by the geosynchronous GOES 13 satellite. TEC and magnetic field both exhibited narrowband, highly regular, quasi-sinusoidal waveforms, with high correlation and coherence indicating a clear link between TEC variations and Pc4 ULF activity. Variations in TEC and 30–50 keV electron flux observed by GOES 13 were also highly correlated and coherent. TEC variations observed directly above Sanikiluaq were in antiphase with eastward magnetic field variations on the ground, while TEC variations observed at the footprint of the GOES 13 satellite were in phase with GOES radial magnetic field and 30–50 keV electron flux. Intermittent occurrence of TEC variations observed by multiple GPS satellites indicated a localized ionospheric response to the Pc4 activity. This is the first clear evidence of a TEC response to these so called “giant pulsations (Pgs).” By applying a multisatellite triangulation technique, the phase velocity, group velocity, and azimuthal wave number of TEC variations were also calculated for an interval of highly coherent measurements. The phase and group propagation velocities were 2–7 km/s and 1–3 km/s north and westward, respectively, while the azimuthal wave number ranged from –35 to –310.

1. Introduction

Total electron content (TEC) measurements of the Global Positioning System (GPS) provide a relatively new and largely unexplored technique for observing the ionospheric response to ultralow frequency (ULF) magnetic field pulsations. Two recent studies [Pilipenko *et al.*, 2014; Watson *et al.*, 2015] have reported modulation of GPS-derived TEC at auroral latitudes by ultralow frequency (ULF) magnetic field pulsations. Pilipenko *et al.* [2014] observed small-amplitude variations in GPS TEC (<1 TECU (total electron content unit, 1 TECU = 10^{16} el m⁻² (TECU)) peak-to-peak amplitude) associated with intense Pc5 band (1.67–6.67 MHz) ULF waves observed on the ground. TEC variations were observed in the afternoon, during the recovery phase of a strong geomagnetic storm. Watson *et al.* [2015] reported large-amplitude (2–7 TECU), GPS TEC variations associated with moderate amplitude, compressional mode Pc5 and Pc6 (<6.67 MHz) variations in the afternoon sector. ULF waves were concurrently observed by geosynchronous satellites and ground magnetometers during a moderate geomagnetic storm.

It has been understood for several decades that ULF waves can impact the ionospheric TEC. By using the carrier phase of satellite-to-ground transmissions of the geostationary ATS 6 satellite, Davies and Hartmann [1976] observed very small-amplitude (<0.002 TECU), quasi-sinusoidal variations in TEC at frequencies of 20–30 MHz. Although no direct correlation was found, the authors suggested that these TEC variations were due to Pc4 magnetic field variations. Using the same measurement technique, Okuzawa and Davies [1981] observed midlatitude variations in TEC at frequencies of 20–100 MHz and amplitudes less than 0.02 TECU. The authors found similar spectral components in TEC variations and simultaneous magnetic field variations observed on the ground. Poole and Sutcliffe [1987] and Liu and Berkey [1993] theoretically explored variations in TEC arising from the influence of ULF waves on the advection and divergence terms of the electron continuity equation for the ionosphere.

ULF waves at Pc4 frequencies characteristic of morningside auroral latitudes are often termed “giant pulsations (Pgs)” [Rostoker *et al.*, 1979; Chisham *et al.*, 1997]. Pg pulsations are mainly observed during periods of low geomagnetic activity [e.g., Motoba *et al.*, 2015] and are most often attributed to particle instabilities

in the magnetosphere [e.g., Chisham, 1996]. They manifest as highly regular, sinusoidal waveforms in ground and satellite magnetometer measurements, typically lasting for 10 min up to several hours [Motoba et al., 2015]. Previous observational studies have attributed Pg activity to even [Takahashi et al., 1992, 2011] and second-order [Chisham and Orr, 1991] harmonics of poloidal mode Alfvén standing waves, potentially resulting from drift-bounce resonance with magnetospheric ions [e.g., Dai et al., 2013]. Dai et al. [2015] recently conducted a statistical study of narrowband, Pc4 poloidal mode waves by using radiation belt space probe observations, which revealed occurrence rates of up to 3.7% on the dayside at $L \sim 4\text{--}5$. Examination of the phase structure of Pg pulsations has generally revealed a westward propagation with a relatively high azimuthal wave number (m) in the range of -10 to -50 [e.g., Chisham et al., 1992; Motoba et al., 2015]. As opposed to the more global Pc5 pulsations observed in previous studies that have used TEC measurements [Pilipenko et al., 2014; Watson et al., 2015], giant pulsations are observed in localized magnetospheric regions, with a highly confined radial extent of $\sim 1 R_E$ [Rostoker et al., 1979; Chisham et al., 1992].

Electromagnetic waves radiated from ULF-induced ionospheric currents can be observed on the ground as signatures of magnetospheric ULF waves. A well-known effect of the ionosphere on Alfvén waves is a rotation of transverse magnetic field perturbations when observed on the ground [e.g., Hughes and Southwood, 1976]. For uniform ionospheric conductivity and perpendicular background magnetic field (relative to the ground), the ground magnetic field perturbation is a signature of the Hall current and is rotated 90° counterclockwise with respect to the ULF wave in the magnetosphere. A second well-known effect is the ionospheric attenuation (i.e., screening) of ULF waves with small azimuthal scales. Hughes [1974] described this “atmospheric shielding effect,” where the wave amplitude on the ground is reduced or completely eliminated.

2. Observations and Analysis

This study makes use of concurrent ground- and satellite-based geomagnetic field measurements and ground-based GPS receiver measurements to examine Pc4 ULF activity and the associated TEC response. TEC is from the Sanikiluaq (56.54°N , 280.77°E geographic coordinates) GPS receiver of the Canadian High Arctic Ionospheric Network (CHAIN) [Jayachandran et al., 2009] and is available at 1 Hz resolution. TEC measurements were detrended using a high band-pass (>0.37 mHz), third-order Butterworth filter. To reduce multipath effects, only TEC from GPS satellites at elevations greater than 25° was considered. TEC measurements are quantified in TEC units (TECUs), where $1 \text{ TECU} = e10^{16} \text{ el m}^{-2}$.

Satellite magnetic field observations are from the fluxgate magnetometer on board the GOES 13 spacecraft, which is located on a geosynchronous orbit at 285.4° east geographic longitude (356.9° magnetic longitude and 12.5° magnetic latitude). High-energy electron (30–100 keV) and proton (80–110 keV) flux measurements of the GOES 13 magnetospheric electron detector (MAGED) and magnetospheric proton detector (MAGPD) are also presented in this study. GOES magnetic field is available at a 2 Hz resolution, while particle flux was sampled at 2 s (electrons) and 16 s (protons). Sanikiluaq magnetic field measurements on the ground were provided by the Canadian Magnetic Observatory System, which is operated by the Geological Survey of Canada. Ground magnetic field is sampled at 1 Hz resolution.

Magnetic field measurements of the GOES 13 satellite were converted to a mean field-aligned coordinate system, similar to measurements presented by Sarris et al. [2009] and Watson et al. [2015]. Coordinate axes (\mathbf{e}_{\parallel} , \mathbf{e}_{φ} , \mathbf{e}_r) were defined by a 45 min running average (\mathbf{B}_{avg}) of the total magnetic field, where \mathbf{e}_{\parallel} is along \mathbf{B}_{avg} , \mathbf{e}_{φ} is at the right angle relative to both \mathbf{e}_{\parallel} and a vector \mathbf{r}_s that runs from the Earth’s center to GOES 13, and \mathbf{e}_r completes the right-handed, orthogonal coordinate system

$$\mathbf{e}_{\parallel} = \frac{\mathbf{B}_{\text{avg}}}{|\mathbf{B}_{\text{avg}}|}, \quad \mathbf{e}_{\varphi} = \mathbf{e}_{\parallel} \times \mathbf{r}_s, \quad \mathbf{e}_r = \mathbf{e}_{\varphi} \times \mathbf{e}_{\parallel} \quad (1)$$

Compressional mode, toroidal (azimuthal) mode, and poloidal (radial) mode pulsations appear in the \mathbf{e}_{\parallel} , \mathbf{e}_{φ} , and \mathbf{e}_r directions, respectively.

Pc4 band GPS TEC variations associated with Pc4 magnetic field variations were observed in the early morning during 07:00–09:30 UTC (02:02–04:31 magnetic local time) on 15 September 2011. This event was observed during a period of low geomagnetic activity ($Dst = -20$, $Kp = 1\text{--}2$) and during recovery from a period of low to moderate auroral activity ($AU = 100$, $AL = -250$). Figure 1 shows magnetic coordinates of

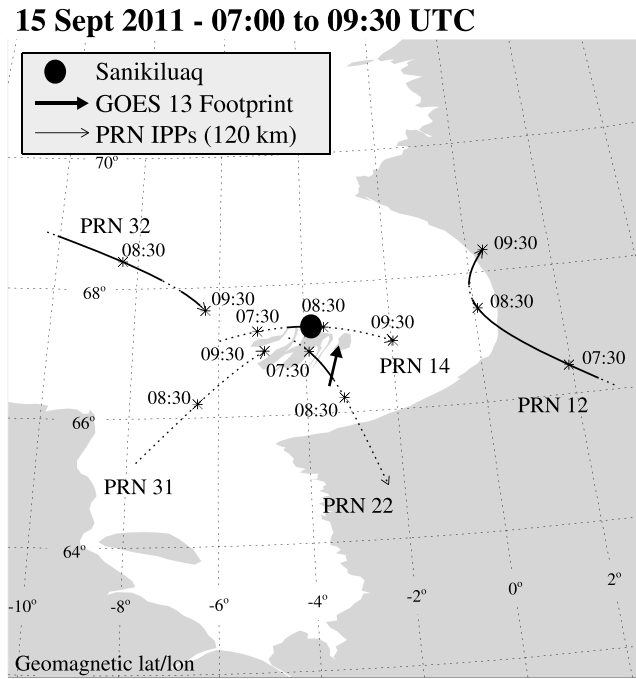


Figure 1. Geomagnetic coordinates of Sanikiluaq, the GOES 13 footprint, and ionospheric pierce points (IPPs) of GPS ray paths at 120 km altitude. Solid black IPP traces indicate where ULF-related TEC variations were observed.

Sanikiluaq, the GOES 13 magnetic footprint, and ionospheric pierce points (IPPs) at 120 km for five GPS satellites over the duration of this Pc4 event. For IPP coordinates, solid black lines indicate periods where GPS satellites observed monochromatic Pc4 band TEC variations closely matching frequencies of Pc4 magnetic field variations. GPS satellites are identified by their PRN number, which refers to each satellite's unique pseudo random noise (PRN) code. Periods where no clear Pc4 band TEC variations were linked to Pc4 magnetic field variations are indicated by dotted lines.

Figure 2 shows (a) magnetic field variations (ΔB) of the GOES 13 satellite in the mean field-aligned coordinate system; (b) electron (e^-) and proton (p^+) flux measurements from telescope 7 of the GOES 13 MAGED and MAGPD, as well as the pitch angle of telescope 7 (dashed line); (c) ground

magnetic field variations (ΔB) from Sanikiluaq in geographic north (X), east (Y), and vertically downward (Z) coordinates; and (d) detrended TEC variations (ΔTEC) from five GPS satellites visible to the Sanikiluaq receiver. A DC offset was added to TEC and magnetic field measurements in order to make the variations more clear. Measurements shown in Figure 3 are in the same format as Figure 2 but with a Pc4 (6.67–22.00 mHz) band-pass filter applied. Variations in electron flux (ΔFlux) are plotted in Figure 3, with a DC offset applied. Similar to Figure 1, periods where TEC variations were linked to Pc4 ULF activity are highlighted in black in Figures 2d and 3d.

Starting around 07:12 UTC, Pc4 variations of up to 2 nT were observed by GOES 13 in all three field-aligned coordinates. Pulsations of about 1 min periodicity continued until 09:15 UTC, with diminishing amplitudes as the event progressed. Field-aligned (B_{\parallel}) variations diminished significantly around 08:05 UTC. Also evident in Figure 2a were longer period (10–25 min) variations in the GOES 13 magnetic field. Wave packets, or periodic (10–25 min) “pulses” of large Pc4 amplitude, were evident in band-pass filtered B_{ϕ} and B_r of Figure 3a. Similar wave packet structuring has been observed in previous Pg pulsation events [e.g., Takahashi *et al.*, 2011]. Also notable is the comparable amplitudes of Pc4 pulsations in the azimuthal and radial directions for most the event. For high- m poloidal waves, magnetospheric MHD models often predict an asymptotic decay of the radial component over time due to a rotation of the wave polarization from radial to azimuthal [e.g., Mann and Wright, 1995]. A similar lack of apparent mode exchange has also been observed in previous Pg events and has been attributed to the continuous driving of the giant pulsation and thus continuous energy source for the poloidal oscillations [Chisham *et al.*, 1997]. Mager and Klimushkin [2013] suggested that trapping of Pg waves in a magnetospheric resonator could explain a number of Pg features, including the sustained poloidal variations and wave packet (amplitude modulation) structure.

As shown in Figures 2b and 3b, significant Pc4 band variations in 30–100 keV electron flux and 80–110 keV proton flux were also observed by GOES 13 from 07:30 to 09:00 UTC. No significant flux variations were observed for electrons >100 keV or protons >110 keV, while lower energy electron (<30 keV) and proton (<80 keV) measurements were not available. Amplitudes of electron and proton flux variations also displayed a periodic character, appearing as wave packets of 10–15 min duration that were simultaneous with similar wave packets in GOES 13 radial (B_r) magnetic field.

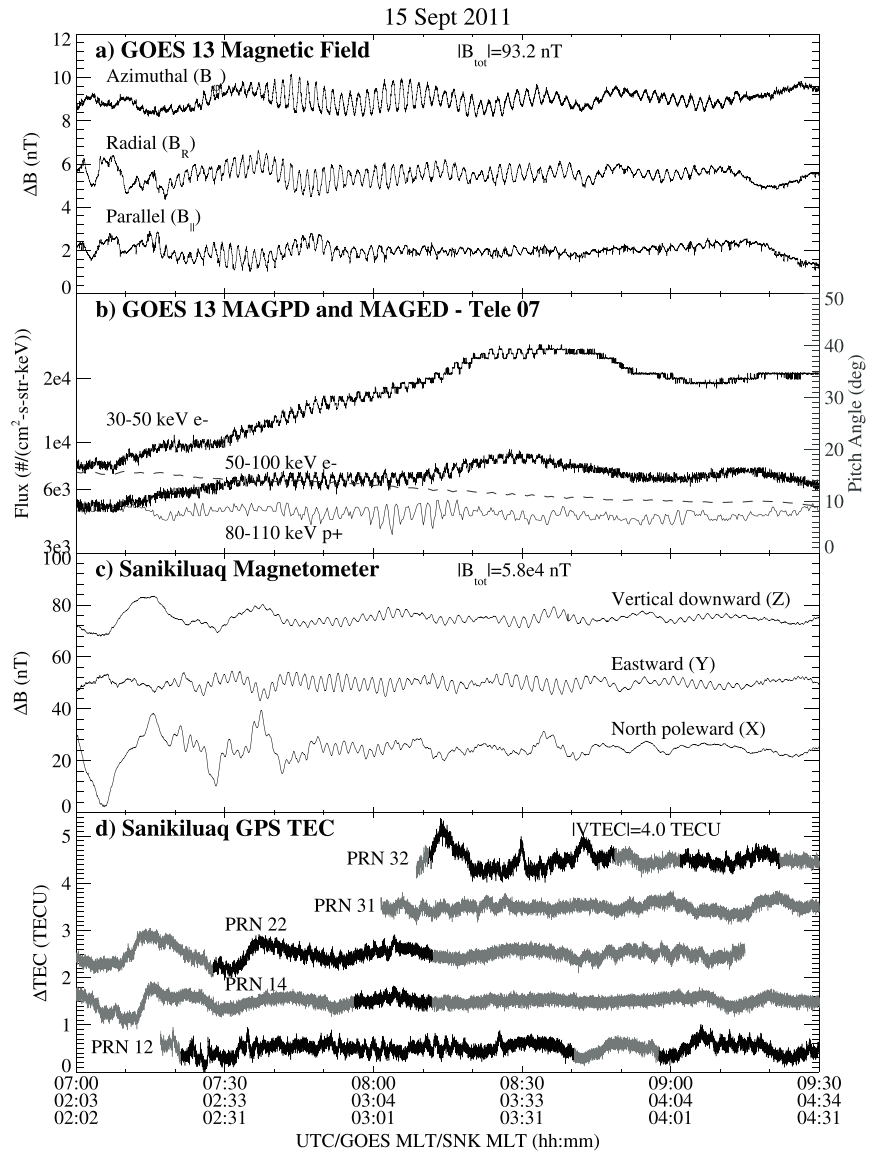


Figure 2. (a) GOES 13 magnetic field variations (ΔB), (b) GOES 13 MAGED electron flux (30–100 keV), MAGPD proton flux (80–110 keV), and pitch angle of telescope 7; (c) Sanikiluaq magnetic field variations (ΔB); and (d) Sanikiluaq GPS TEC variations (Δ TEC). A DC shift was applied to magnetic field and TEC measurements for visualization purposes. TEC measurements plotted in black indicate where ULF-related TEC variations were observed.

As shown in Figures 2c and 3c, Pc4 waves of up to 6 nT were detected by the Sanikiluaq magnetometer starting at 07:15 UTC, concurrent with the onset of Pc4 variations at GOES 13. Pc4 activity was evident in each magnetic field component, lasting until 09:15 UTC in eastward (Y) and downward (Z) directions while diminishing around 08:45 UTC in the poleward (X) direction. Ground Pc4 signatures also manifested as wave packets of 10–25 min duration, which roughly coincided with wave packets observed in the GOES 13 radial (B_R) magnetic field and 30–100 keV electron and 80–110 keV proton flux.

As shown in Figures 2d and 3d, variations in GPS TEC with peak-to-peak amplitudes of up to 0.35 TECU were observed by several GPS satellites. Occurrence of narrowband TEC variations with frequencies closely matching those of Pc4 magnetic field variations was intermittent and varied from satellite to satellite. Referring to IPP coordinates in Figure 1, Pc4 band TEC variations were first observed around 07:20 UTC by PRN 12, the easternmost satellite. Variations were observed almost continuously by PRN 12 until 09:30 UTC, as the satellite tracked to the northeast of Sanikiluaq. Similar to magnetic field variations, TEC variations appeared in

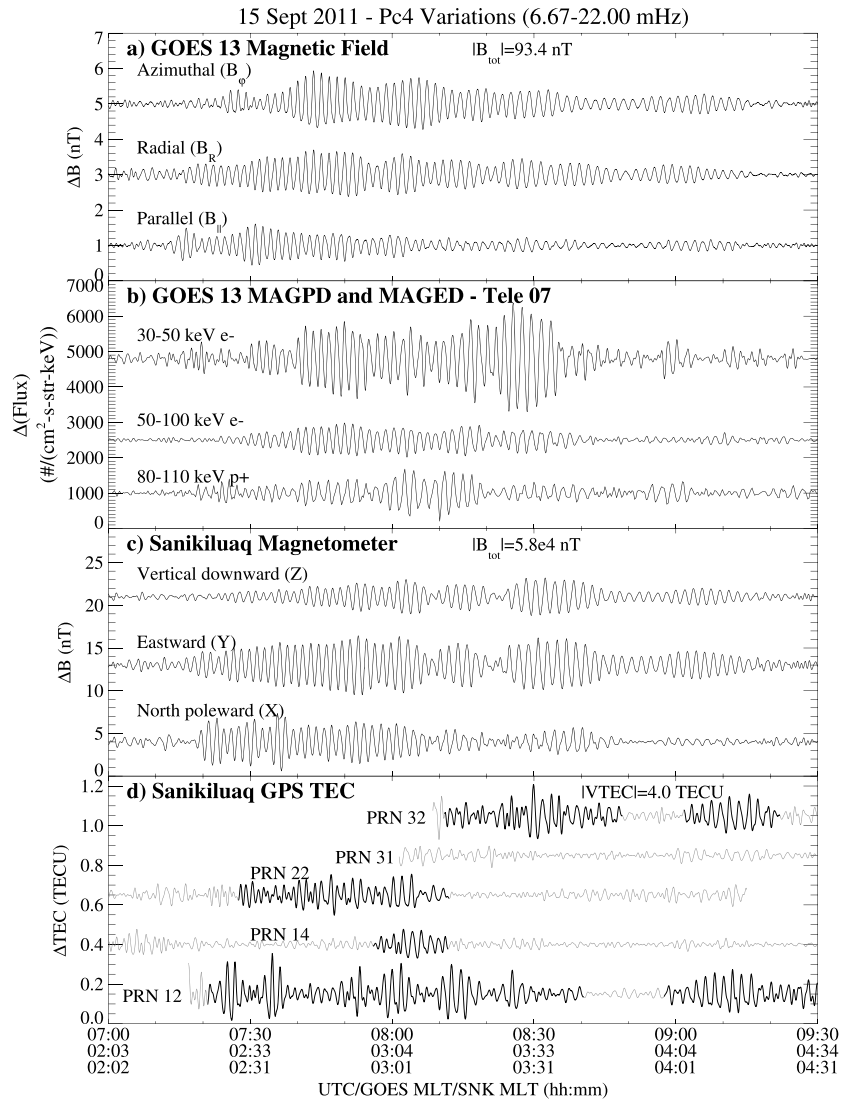


Figure 3. Same format as Figure 2, with a Pc4 (6.67–22.00 mHz) third-order Butterworth band-pass filter applied. Particle flux variations (Δ Flux) are shown in Figure 3b.

pulses of high amplitude but with shorter 5–10 min durations. PRN 32, located to the northwest of Sanikiluaq, observed TEC variations for a large portion of the interval 08:10–09:22 UTC. PRN 14, which provided TEC measurements for the entire event, observed clear Pc4 signatures only during 07:55–08:12 UTC, as it tracked directly overhead Sanikiluaq. PRN 22 observed clear, monochromatic variations from 07:28 to 08:11 UTC, with no clear variations observed when the satellite progressed to more southern latitudes. PRN 31, located to the southwest of Sanikiluaq, observed no clear Pc4 TEC variations related to Pc4 magnetic field activity. These multisatellite observations indicate that the TEC response to Pc4 activity expanded westward, with a more steady ionospheric response to the east and northwest of Sanikiluaq and little to no response to the south of Sanikiluaq. Note that the GOES 15 satellite, located 15° to the west of GOES 13, observed similar Pc4 activity at a delay of ~17 min, while ground magnetometer stations (Gilliam and Fort Churchill) located 25° to the west of Sanikiluaq observed no significant Pc4 activity. Since the corotation speed of GOES satellites is only 0.25° per minute, the ~17 min delay indicates an apparent westward propagation of Pc4 activity at the geosynchronous orbit. A westward phase propagation is a characteristic of Pg events, and there is past observational evidence to suggest that this reflects the bounce resonance [Chisham *et al.*, 1992] or drift resonance [Dai *et al.*, 2013] of Pc4 waves with westward drifting ring current ions.

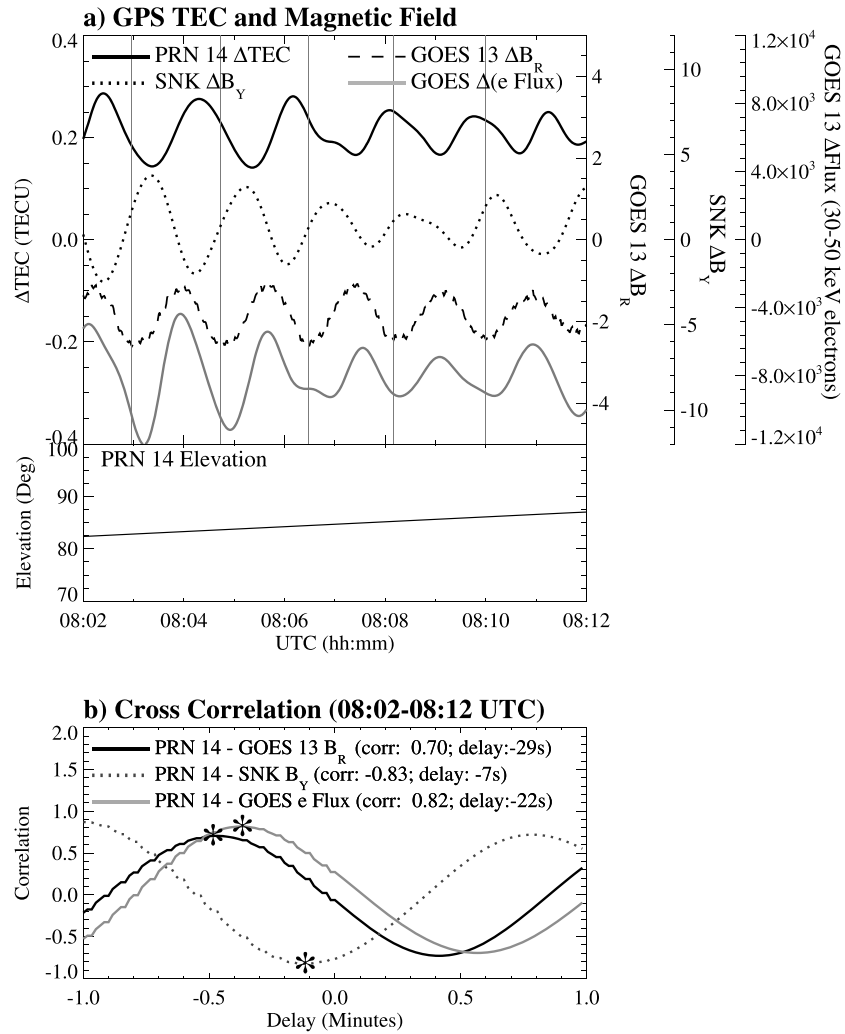


Figure 4. (a) Pc4 band-pass filtered PRN 14 ΔTEC , GOES 13 ΔB_R , Sanikiluaq ΔB_Y , and GOES 13 30–50 keV electron flux, in addition to PRN 14 satellite elevation. (b) Cross correlation of PRN 14 TEC with GOES 13 B_R , Sanikiluaq B_Y , and GOES 13 electron flux.

Figure 4 shows cross-correlation analysis of PRN 14 TEC with GOES 13 B_R , Sanikiluaq B_Y , and GOES 13 30–50 keV electron flux for 08:02–08:12 UTC. PRN 14 was almost directly overhead Sanikiluaq during this interval. Figure 4a plots GOES 13 ΔB_R and electron flux variations, Sanikiluaq ΔB_Y , and ΔTEC and satellite elevation of PRN 14. Similar quasi-sinusoidal and highly regular waveforms are evident in TEC, magnetic field, and electron flux measurements. Figure 4b shows cross correlation of unfiltered PRN 14 TEC from 08:02 to 08:12 UTC, with sliding 10 min windows of GOES 13 B_R (black), Sanikiluaq B_Y (dotted line), and GOES 13 electron flux (grey). Peak correlations are marked with an asterisk and are listed in the figure along with the corresponding time delays. A negative delay indicates that variations in PRN 14 TEC lag behind the corresponding magnetic field or flux variations. High anticorrelation of -0.83 between PRN 14 TEC and Sanikiluaq B_Y was found at a delay of -7 s, indicating that variations in TEC and eastward magnetic field were approximately 180° out of phase. Sanikiluaq B_X (not shown) and PRN 14 TEC were close to in phase over this interval. PRN 14 TEC was highly correlated with GOES 13 B_R (0.7) and 30–50 keV electron flux (0.82) at a delay of -29 s and -22 s and anticorrelated at delay of 25 s and 32 s, respectively, and thus, the phase relationship between these variations was unclear. Visual examination of PRN 14 TEC and GOES 13 electron flux in Figure 4a reveals remarkably similar waveforms. There was insignificant correlation (<0.5) between PRN 14 TEC and 80–110 keV proton flux over this time interval (not shown).

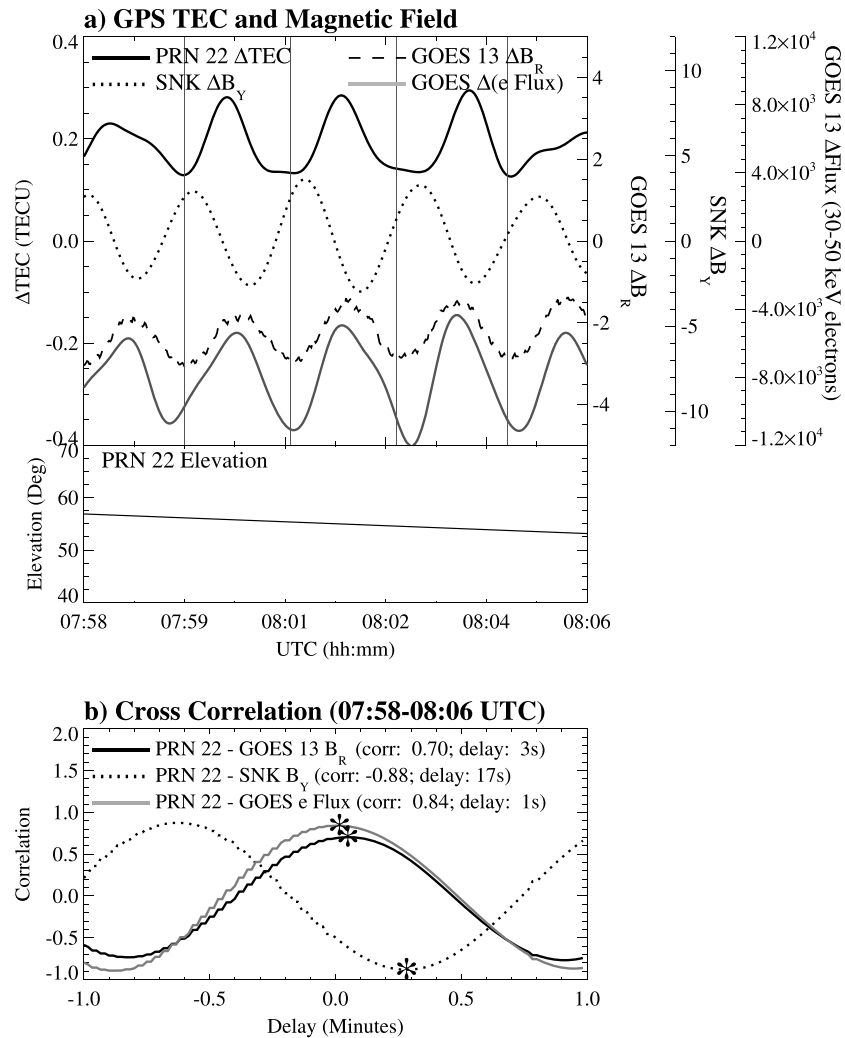


Figure 5. Cross-correlation analysis using PRN 22 TEC for 07:58–08:06 UTC, in the same format as Figure 4.

Figure 5 shows similar correlation analysis for PRN 22 TEC and magnetic field/electron flux measurements for 7:58–8:06 UTC, when the PRN 22 IPP was in close proximity to the GOES 13 footprint. Variations in PRN 22 TEC were similar to variations in GOES 13 B_r , Sanikiluaq B_y , and GOES 13 30–50 keV electron flux, with correlations of 0.70, -0.88 , and 0.84 at delays of 3 s, 17 s, and 1 s, respectively. Note that the PRN 22 TEC variations, GOES 13 magnetic field variations, and GOES 13 electron flux variations are very close to in phase during this time interval. The relative phase between PRN 22 TEC variations and magnetic field/flux variations differs from phase delays observed in Figure 4, indicating that the phase of TEC variations has a significant spatial variation. The relative phase of TEC variations is further examined in Figure 8. There was significant correlation (0.74) between PRN 22 TEC and GOES 13 80–110 keV proton flux during this time interval, at a time delay of 24 s (not shown).

In the interest of investigating a possible drift-bounce resonance generating the observed Pc4 pulsations, the relative phase of GOES 13 B_r and proton flux variations was also examined (not shown). While magnetic field and ion flux variations are expected to be in quadrature for resonance mechanisms [e.g., Dai et al., 2013], no consistent phase relationship was observed between GOES 13 B_r and 80–110 keV proton flux from any of the nine MAGPD telescopes during the event, and thus, no evidence of drift-bounce resonance was observed. The presence of undetected resonant protons at lower energies (<80 keV) is possible, as was observed by Chisham et al. [1992], while some aliasing effects may have been present in the 16 s resolution GOES 13 proton flux data.

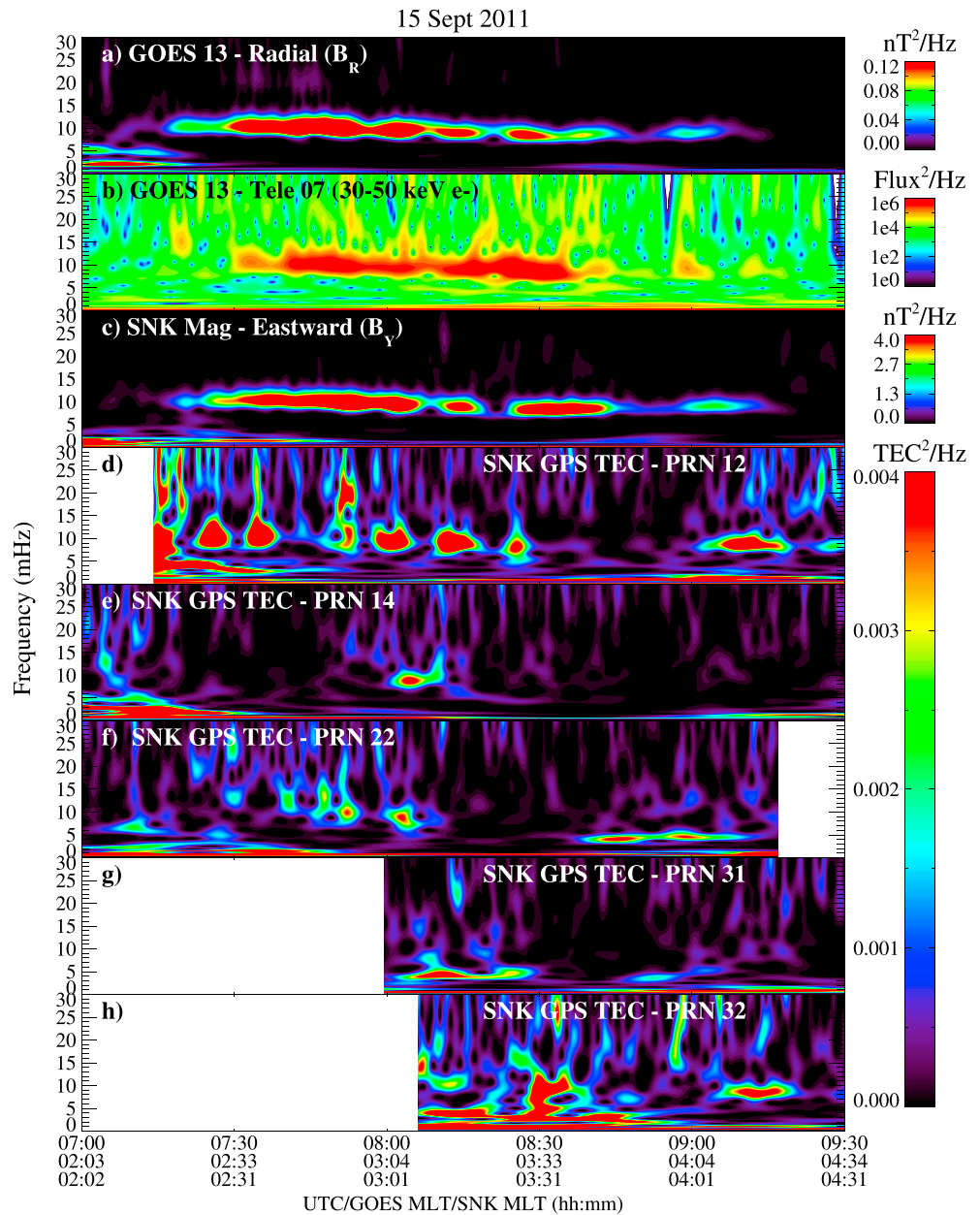


Figure 6. Dynamic power spectra of (a) GOES 13 radial (B_r) magnetic field, (b) GOES 13 30–50 keV electron flux measurements of telescope 7, (c) Sanikiluaq eastward (Y) magnetic field, and (d–h) Sanikiluaq GPS TEC.

As shown in Figures 4 and 5, variations in GOES 13 B_r lead variations in Sanikiluaq B_Y by 28°–37° (while accounting for the 90° counterclockwise rotation of the wave polarization), which is consistently the case throughout the event. Referring to Figure 1, the longitudinal separation between Sanikiluaq and the GOES 13 footprint is 0.6°–0.8° during the event, which corresponds to an azimuthal wave number in the range of –35 to –62. This agrees with previous wave number estimates for Pg events [Chisham *et al.*, 1992; Motoba *et al.*, 2015]. Given the latitudinal separation of Sanikiluaq and the GOES 13 footprint (0.3°–0.7°), there is a possible latitudinal component to the phase shift that has not been accounted for in this estimation of the azimuthal wave number.

Figure 6 shows 0–30 mHz dynamic power spectra of (a) GOES 13 radial (B_r) magnetic field, (b) electron flux for energies of 30–50 keV, (c) eastward (Y) magnetic field on the ground in Sanikiluaq, and (d)–(h) GPS TEC for

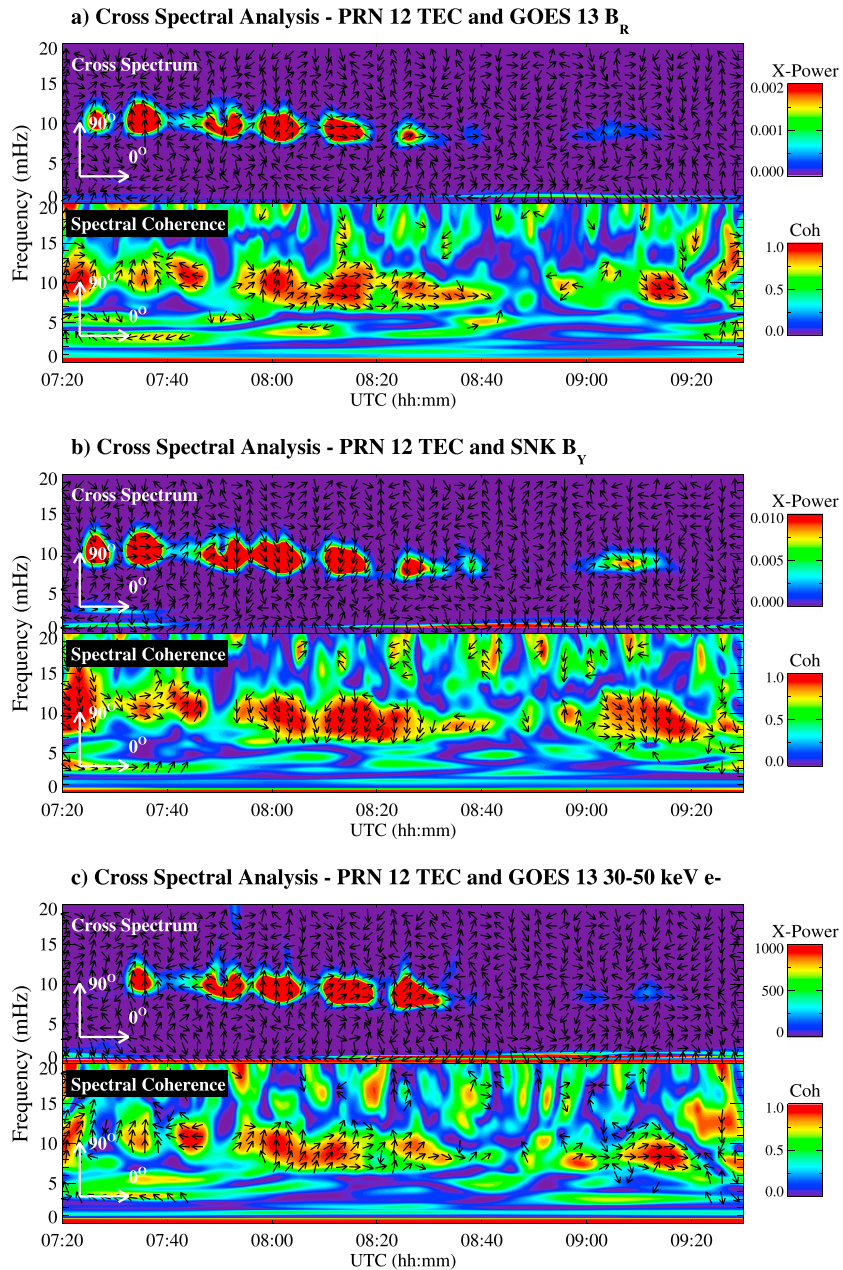


Figure 7. Cross-dynamic spectral power and magnitude squared coherence for (a) PRN 12 TEC and GOES 13 radial (B_R) magnetic field, (b) PRN 12 TEC and Sanikiluaq eastward (Y) magnetic field, and (c) PRN 12 TEC and GOES 13 30–50 keV electron flux of telescope 7. Arrows show cross phase of TEC and magnetic field/flux variations.

multisatellite measurements shown in Figure 2d. Dynamic power spectra were calculated using the S transform [Stockwell *et al.*, 1996]. As seen in Figures 6a–6c, magnetic field and electron flux variations were dominated by a narrow band of frequencies in the range of 9.5–10.5 mHz. Other components in GOES 13 and Sanikiluaq magnetic field measurements were dominated by the same narrow band of frequencies. The dynamic power spectrum for 80–110 keV protons observed by GOES 13 (not shown) revealed a narrow band of frequencies around 8.0–9.0 mHz, slightly lower than dominant frequencies of GOES 13 magnetic field and electron flux variations. A notable feature in the dynamic power spectrum for GOES 13 variations (Figure 6a) was a narrowband frequency of ~21 mHz observed from 07:25 to 07:53 UTC, which indicates a possible higher harmonic associated with resonant variations of magnetic field lines.

In Figures 6d–6h, intermittent, narrowband frequency components closely matching magnetic field and electron flux frequencies are evident in TEC dynamic power spectra. Intervals where TEC frequencies closely matched those of magnetic field variations are highlighted in Figures 1–3. No clear Pc4 frequency components related to Pc4 magnetic field variations were observed in the PRN 31 TEC dynamic power spectrum.

Figure 7 shows cross-spectral analysis of PRN 12 TEC with (a) GOES 13 B_r , (b) Sanikiluaq B_y , and (c) GOES 13 30–50 keV electron flux of telescope 7. Color contours in Figures 7a–7c show the cross-spectral power and magnitude squared coherence of the dynamic power spectra, while arrows in Figures 7a–7c indicate the relative phase between TEC and magnetic field/flux variations. An arrow pointing right indicates in-phase variations, while an arrow pointing up indicates that PRN 12 TEC is 90° ahead in phase. In coherence plots, relative phase is shown only where coherence was greater than 0.6. The cross-spectral power highlights common spectral components in the two time series, while the coherence highlights phase-locked variations in time-frequency space. This cross-spectral analysis technique is discussed in detail by *Grinsted et al.* [2004], with similar analysis carried out by *Pilipenko et al.* [2014] and *Watson et al.* [2015]. Cross-spectral analysis clearly indicates a link between PRN 12 TEC variations and Pc4 ULF waves observed by GOES 13 and Sanikiluaq magnetometers, with intermittent periods of high common power at Pc4 ULF wave frequencies throughout the event and high coherence at these same frequencies.

In order to examine the local phase structure of TEC variations in the Pc4 band, the cross phase of TEC variations observed by three GPS satellites was examined for 07:51–08:07 UTC. Narrowband, coherent Pc4 band TEC variations were observed by PRNs 12, 14, and 22 during this time interval. Shown in Figure 8 are (a) PRN IPP locations at 110 km altitude for the 16 min interval, (b) Pc4 band-pass filtered TEC, (c)–(e) coherence and cross phase for each combination of TEC measurements, where an arrow pointing up indicates that PRN 14 TEC (c) or PRN 22 TEC (d)–(e) is 90° ahead in phase, (f) apparent phase (dashed lines) and group (solid lines) propagation speeds of TEC variations between each pair of IPPs, and (g) latitudinal (blue), longitudinal (red), and total (black) phase and group propagation speeds of TEC variations, calculated using a triangulation technique discussed below. The azimuthal wave number (dotted line) was calculated from the longitudinal component of the phase variation (f).

In Figure 8f, the apparent phase propagation velocities ($\mathbf{v}_{i,j \text{ phase}}$) between IPPs of PRNs i,j were calculated using

$$\mathbf{v}_{i,j \text{ phase}} = \frac{\mathbf{d}_{i,j}}{\Delta t_{i,j}} \quad (2)$$

where $\mathbf{d}_{i,j}$ is the displacement between IPPs i,j and $\Delta t_{i,j}$ is the propagation time of TEC variations between IPPs i,j . Phase velocity was calculated at 9.7 mHz (peak spectral power), only when the cross-spectral coherence in Figures 8c–8e was >0.6 . Propagation time was calculated from the relative phase $\Delta\phi_{i,j}$ of TEC variations shown in Figures 8c–8e using

$$\Delta t_{i,j} = \frac{\Delta\phi_{i,j} + 2\pi N}{2\pi f} \quad (3)$$

where f is the frequency of TEC variations and N is the number of full integer cycles that TEC variations undergo as they propagate between two IPPs. For all calculations it was assumed that $N=0$. The apparent group propagation velocity ($\mathbf{v}_{i,j \text{ group}}$) between each IPP pair i,j was calculated from the dispersion characteristics of the TEC waveforms, similar to the analysis technique used by *Chisham and Mann* [1999] to calculate the group propagation speed of a high- m Pc5 wave observed by a network of ground magnetometers. The apparent wave number ($k_{i,j}$) for each IPP pair is simply

$$k_{i,j}(f) = \frac{\Delta\phi_{i,j}(f)}{d_{i,j}} \quad (4)$$

which varies with frequency f as seen in Figures 8c–8e. At times where $k_{i,j}$ had an approximate linear variation with frequency, and the coherence of TEC variations observed by PRNs i,j was >0.6 , the apparent group speed for each IPP pair was calculated as

$$v_{i,j \text{ group}} = \frac{\Delta\omega}{\Delta k_{i,j}} \quad (5)$$

where $\omega = 2\pi f$.

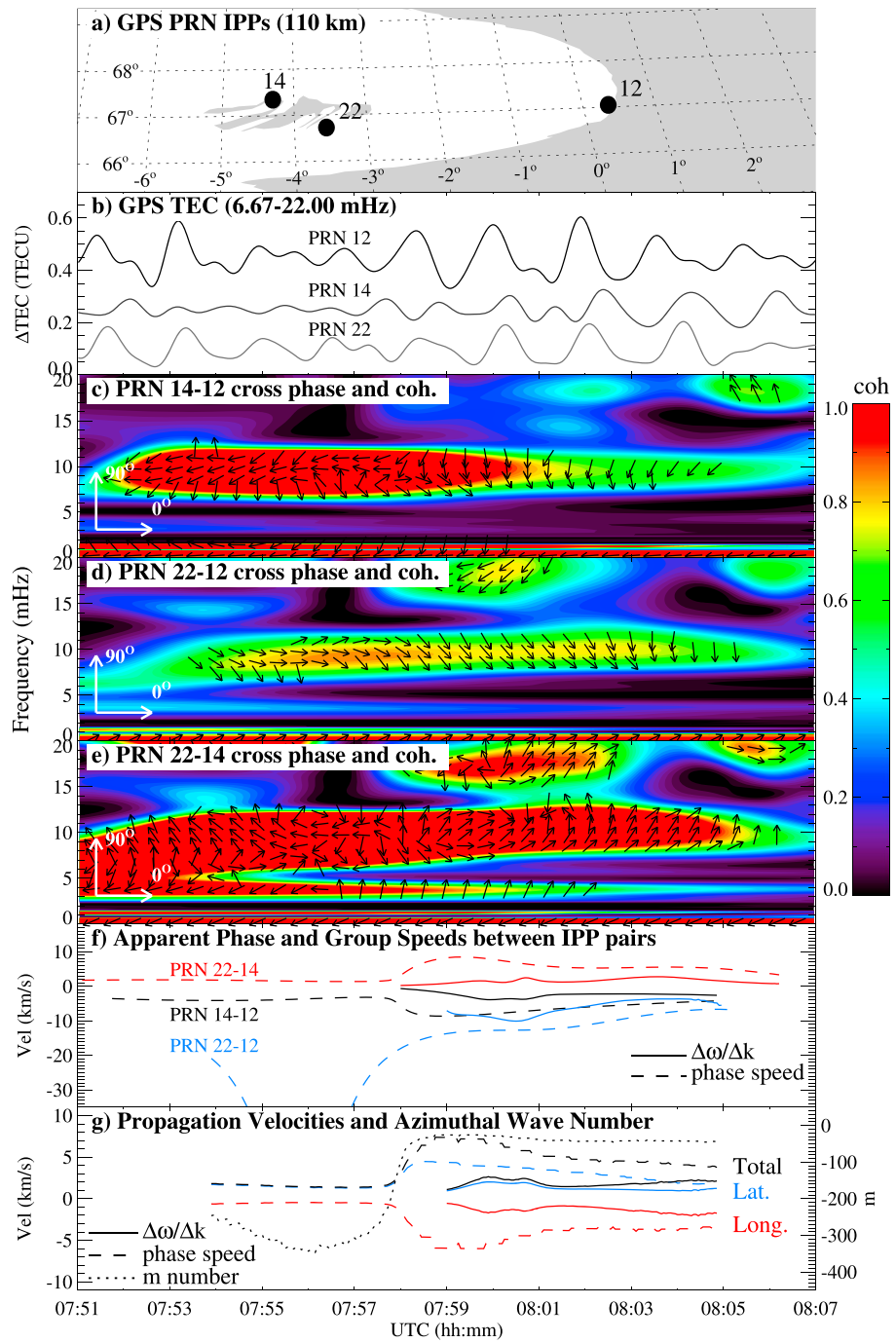


Figure 8. Cross-phase analysis of TEC variations observed by PRNs 12, 14, and 22 for 07:51–08:07 UTC: (a) PRN IPPs at 110 km altitude, (b) Δ TEC filtered in the Pc4 frequency band, (c–e) cross phase and spectral coherence for each combination of TEC measurements, (f) apparent phase and group propagation speeds on straight line paths between IPP pairs, and (g) phase velocity, group velocity, and azimuthal wave number of TEC variations estimated using a triangulation technique discussed in the text.

Longitudinal and latitudinal phase and group velocities shown in Figure 8g were calculated using a triangulation technique that has been applied in previous TEC observations of propagation ionospheric structures [Watson et al., 2011; Jayachandran et al., 2011; Watson et al., 2015]. Details of the technique are discussed in Watson et al. [2015]. In this technique, the magnitude ($|\mathbf{v}_{prop}$) and direction (\mathbf{e}_{prop}) of phase and group

propagation velocities are estimated from projections of apparent propagation velocities (\mathbf{v}_{ij}) between PRN IPP pairs

$$|\mathbf{v}_{\text{prop}}| = \mathbf{v}_{i,j} \cdot \mathbf{e}_{\text{prop}} \quad (6)$$

where for TEC observations from three GPS satellites, the three possible velocities \mathbf{v}_{ij} are applied to equation (6) to determine the best estimate of \mathbf{v}_{prop} . Azimuthal wave number in Figure 8g was calculated from the longitudinal component of the phase propagation and is defined as the change in degree phase per degree longitude (negative for westward propagation).

In Figure 8f, positive phase and group velocities for propagation from PRN 22 to PRN 14 and negative velocities for propagation from PRN 14 to PRN 12 and PRN 22 to PRN 12 indicate a consistent westward and northward propagation during the 16 min time interval. Group velocities were only calculated during 07:58–08:08 UTC, when frequency changed linearly with wave number. As observed in Figures 8c–8e, sudden changes in relative phase of TEC variations occur during ~07:56–07:59 UTC, resulting in the sudden change in apparent phase propagation velocities in Figure 8f. Phase propagation velocity in Figure 8g shows a primarily northward propagation of ~2 km/s for ~07:54–07:58 UTC, with an azimuthal wave number of ~–240 to ~–310 reflecting the small longitudinal component (~–0. km/s) of the propagation. During the change in relative phase of TEC variations, phase propagation velocity increased to ~6 km/s westward and ~4 km/s northward at 07:59 UTC, followed by a steady decrease to ~4 km/s westward and ~2 km/s northward at 08:05 UTC. The azimuthal wave number varied from ~–20 to ~–40 over this interval. Before the shift in relative phase, the latitudinal component of the phase shift was 180°–230° over the ~0.8° latitudinal range of IPPs in Figure 8a and 90°–160° after the phase shift. Calculated group velocities at ~07:59 UTC were ~0.5 km/s westward and 0.9 km/s northward, with a net increase to ~2 km/s westward and ~2 km/s northward at 08:05 UTC.

The assumption that ionization resulting in observed TEC variations occurs at 110 km, and thus the choice of IPP altitude at 110 km for calculation of propagation velocities, will impact the magnitude of calculated phase and group propagation velocities, but not the direction. For example, an assumption that ionization occurs at 270 km altitude in the *F* region will result in phase propagation speeds of ~3–18 km/s, group speeds of ~3–6 km/s, and azimuthal wave numbers ranging from ~–10 to ~–153 during the time interval 07:54–08:05 UTC. No measurements from all sky imagers, riometers, ionosondes, etc., were available in Sanikiluaq during this event to help determine the altitude of ionization.

The longitudinal phase propagation and azimuthal wave number (~–20 to ~–40) of TEC variations for 07:59–08:05 UTC is in the range of previous estimates for Pg waves [Chisham *et al.*, 1992; Motoba *et al.*, 2015] and is also close to the *m* number estimated from magnetic field measurements of GOES 13 and Sanikiluaq magnetometers for this event (~–35 to ~–62). As noted previously, this estimate did not account for a possible latitudinal contribution to the relative phase of magnetic field variations. There was also a significant northward component (radial in the magnetosphere) to the phase propagation of TEC variations, which may partially reflect the latitudinal structure of field line resonance. The local phase structure of TEC variations associated with the giant pulsations varied significantly during the event, and further analysis is required to find a physical interpretation of the phase structure and its evolution over time and to resolve spatial and temporal variations in TEC. Further study is also needed to determine if and how the phase structure of TEC variations accurately reflects the phase structure and propagation of the ULF wave itself. Although the physical interpretations of the results shown in Figure 8 are not clear, this figure demonstrates the potential applicability of the GPS TEC technique in the high-resolution study of high-*m* giant pulsations and other ULF waves.

3. Discussion and Conclusions

Variations in GPS-derived TEC were attributed to narrowband, low-intensity Pc4 ULF wave activity. Characteristics of Pc4 ULF waves were consistent with previous descriptions of giant pulsations (Pgs) often observed in the early morning auroral ionosphere. During observed Pc4 activity, small-amplitude (0.05–0.35 TECU peak-to-peak amplitude), highly sinusoidal waveforms were observed in TEC measurements of multiple GPS satellites. Cross correlation and cross-spectral analysis revealed high correlation and coherence between TEC and magnetic field variations, indicating that TEC variations were clearly linked to Pc4 ULF activity. Multisatellite observations of intermittent TEC variations indicated that the

ionospheric response to Pc4 activity was highly localized and that the phase of the TEC response varied sharply with latitude and local time. TEC variations observed directly overhead Sanikiluaq were approximately in antiphase with eastward (B_y) magnetic field variations observed by the Sanikiluaq magnetometer, while TEC variations observed near the footprint of the GOES 13 satellite were approximately in phase with variations in magnetic field (B_z component) and 30–50 keV electron flux observed by GOES 13. This is the first clear observation of TEC variations associated with giant pulsations (Pgs).

Peak-to-peak amplitudes of TEC variations associated with Pc4 waves were in the range of 0.05–0.35 TECU, which corresponds to a fractional disturbance ($\Delta\text{TEC}/\text{TEC}$) of 2%–8% relative to the 3–5 TECU estimated background TEC during this event. Using theoretical considerations, *Pilipenko et al.* [2014] outlined a number of mechanisms by which the wave action on the ionosphere could produce fractional TEC variations of up to ~1.0%, significantly smaller than the fractional variations observed here. One possible mechanism to explain the TEC response to Pc4 waves is the wave-modulated precipitation of energetic particles. *Hillebrand et al.* [1982] observed modulation of 30–50 keV electron flux by giant pulsations, which they suggested would produce periodic ionization of the *D* region ionosphere and *E* region ionosphere. *Chisham et al.* [1992] also discussed Pg modulation of energetic particle precipitation by replenishment of the atmospheric loss cone through pitch angle diffusion. In this study, TEC variations showed high correlation and coherence with 30–50 keV electron flux observed by GOES 13; however, this is not sufficient evidence that wave-modulated electron precipitation resulted in observed variations in TEC.

Multisatellite measurements and a simple triangulation technique were also used to estimate the local phase and dispersion characteristics of TEC variations associated with giant pulsations. For an 11 min interval where coherent, multisatellite TEC variations were observed, TEC variations were found to initially propagate mainly poleward, followed by a poleward and westward propagation due to a shift in relative phase of TEC variations. Assuming ionization of the *E* region ionosphere, TEC variations had a phase speed of ~2 km/s and an azimuthal wave number of –240 to –310 before the phase shift and a phase speed of 4–7 km/s and an azimuthal wave number of –20 to –40 after the phase shift. A group propagation speed of 1–3 km/s was also calculated after the phase shift. The azimuthal wave number estimated from GOES 13 satellite and Sanikiluaq ground magnetic field variations was –35 to –62. As demonstrated for this event, the GPS TEC technique is a potentially useful tool for observing the local structure of giant pulsations and other high-*m* ULF waves, which may be unobservable by measurement techniques with lower spatial resolutions such as ground magnetometer arrays. Further analysis is required to physically interpret the phase structure of TEC variations and whether it accurately reflects the phase structure and propagation of the ULF wave.

The significant TEC response to low-intensity Pc4 ULF activity is an important addition to the existing observational picture of ULF wave interaction with the ionosphere. Further development of techniques such as cross-phase analysis may be useful for examining the phase structure or propagation of TEC waveforms in a relatively localized region of the ionosphere.

Acknowledgments

CHAIN infrastructure was funded by the Canadian Foundation for Innovation and the New Brunswick Innovation Foundation. CHAIN operates in collaboration with Canadian Space Agency. The Natural Sciences and Engineering Research Council of Canada provides science funding for CHAIN. CHAIN data are available online through <http://chain.physics.ubc.ca>.

References

- Chisham, G. (1996), Giant pulsations: An explanation for their rarity and occurrence during geomagnetically quiet times, *J. Geophys. Res.*, *101*(A11), 24,755–24,763, doi:10.1029/96JA02540.
- Chisham, G., and I. R. Mann (1999), A Pc5 ULF wave with large azimuthal wavenumber observed within the morning sector plasmasphere by Sub-Auroral Magnetometer Network, *J. Geophys. Res.*, *104*(A7), 14,717–14,727, doi:10.1029/1999JA900147.
- Chisham, G., and D. Orr (1991), Statistical studies of giant pulsations (Pgs): Harmonic mode, *Planet. Space Sci.*, *39*(7), 999–1006, doi:10.1016/0032-0633(91)90105-J.
- Chisham, G., D. Orr, and T. K. Yeoman (1992), Observations of a giant pulsation across an extended array of ground magnetometers and on auroral radar, *Planet. Space Sci.*, *40*(7), 953–964, doi:10.1016/0032-0633(92)90135-B.
- Chisham, G., I. R. Mann, and D. Orr (1997), A statistical study of giant pulsation latitudinal polarization and amplitude variation, *J. Geophys. Res.*, *102*(A5), 9619–9629, doi:10.1029/97JA00325.
- Dai, L., et al. (2013), Excitation of poloidal standing Alfvén waves through drift resonance wave-particle interaction, *Geophys. Res. Lett.*, *40*, 4127–4132, doi:10.1002/grl.50800.
- Dai, L., et al. (2015), Storm time occurrence and spatial distribution of Pc4 poloidal ULF waves in the inner magnetosphere: A Van Allen Probes statistical study, *J. Geophys. Res. Space Physics*, *120*, 4748–4762, doi:10.1002/2015JA021134.
- Davies, K., and G. K. Hartmann (1976), Short-period fluctuations in total columnar electron content, *J. Geophys. Res.*, *81*(19), 3431–3434, doi:10.1029/JA081i019p03431.
- Grinsted, A., J. C. Moore, and S. Jevrejeva (2004), Application of the cross wavelet transform and wavelet coherence to geophysical time series, *Nonlinear Processes Geophys.*, *11*, 561–566, doi:10.5194/npg-11-561-2004.
- Hillebrand, O., J. Muench, and R. L. McPherron (1982), Ground-satellite correlative study of a giant pulsation event, *J. Geophys.*, *51*(2), 129–140.

- Hughes, W. J. (1974), The effect of the atmosphere and ionosphere on long period magnetospheric micropulsations, *Planet. Space Sci.*, *22*, 1157–1172.
- Hughes, W. J., and D. J. Southwood (1976), The screening of micropulsation signals by the atmosphere and ionosphere, *J. Geophys. Res.*, *81*(19), 3234–3240, doi:10.1029/JA081i019p03234.
- Jayachandran, P. T., et al. (2009), Canadian High Arctic Ionospheric Network (CHAIN), *Radio Sci.*, *44*, R50A03, doi:10.1029/2008RS004046.
- Jayachandran, P. T., C. Watson, I. J. Rae, J. W. MacDougall, D. W. Danskin, R. Chadwick, T. D. Kelly, P. Prikryl, K. Meziane, and K. Shiokawa (2011), High-latitude GPS TEC changes associated with a sudden magnetospheric compression, *Geophys. Res. Lett.*, *38*, L23104, doi:10.1029/2011GL050041.
- Liu, J. Y., and F. T. Berkey (1993), Oscillations in ionospheric virtual height, echo amplitude and Doppler velocity: Theory and observations, *J. Geomag. Geoelectr.*, *45*, 207–217.
- Mager, P. N., and D. Y. Klimushkin (2013), Giant pulsations as modes of a transverse Alfvénic resonator on the plasmopause, *Earth Planets Space*, *65*, 397–409.
- Mann, I. R., and A. N. Wright (1995), Finite lifetimes of ideal poloidal Alfvén waves, *J. Geophys. Res.*, *100*(A12), 23,677–23,686, doi:10.1029/95JA02689.
- Motoba, T., K. Takahashi, J. V. Rodriguez, and C. T. Russell (2015), Giant pulsations on the afternoonside: Geostationary satellite and ground observations, *J. Geophys. Res. Space Physics*, *120*, 8350–8367, doi:10.1002/2015JA021592.
- Okuzawa, T., and K. Davies (1981), Pulsations in total columnar electron content, *J. Geophys. Res.*, *86*(A3), 1355–1363, doi:10.1029/JA086iA03p01355.
- Pilipenko, V., V. Belakhovsky, D. Murr, E. Fedorov, and M. Engebretson (2014), Modulation of total electron content by ULF Pc5 waves, *J. Geophys. Res. Space Physics*, *119*, 4358–4369, doi:10.1002/2013JA019594.
- Poole, A. W. V., and P. R. Sutcliffe (1987), Mechanisms for observed total electron content pulsations at mid latitudes, *J. Atmos. Terr. Phys.*, *49*(3), 231–236, doi:10.1016/0021-9169(87)90058-4.
- Rostoker, G., H.-L. Lam, and J. V. Olson (1979), PC 4 giant pulsations in the morning sector, *J. Geophys. Res.*, *84*(A9), 5153–5166, doi:10.1029/JA084iA09p05153.
- Sarris, T., X. Li, and H. J. Singer (2009), A long-duration narrowband Pc5 pulsation, *J. Geophys. Res.*, *114*, A01213, doi:10.1029/2007JA012660.
- Stockwell, R. G., L. Mansinha, and R. P. Lowe (1996), Localization of the complex spectrum: The S transform, *IEEE Trans. Signal Process.*, *44*, 988–1001.
- Takahashi, K., N. Sato, J. Warnecke, H. Lühr, H. E. Spence, and Y. Tonegawa (1992), On the standing wave mode of giant pulsations, *J. Geophys. Res.*, *97*(A7), 10,717–10,732, doi:10.1029/92JA00382.
- Takahashi, K., K.-H. Glassmeier, V. Angelopoulos, J. Bonnell, Y. Nishimura, H. J. Singer, and C. T. Russell (2011), Multisatellite observations of a giant pulsation event, *J. Geophys. Res.*, *116*, A11223, doi:10.1029/2011JA016955.
- Watson, C., P. T. Jayachandran, E. Spanswick, E. F. Donovan, and D. W. Danskin (2011), GPS TEC technique for observation of the evolution of substorm particle injection, *J. Geophys. Res.*, *116*, A00190, doi:10.1029/2010JA015732.
- Watson, C., P. T. Jayachandran, H. J. Singer, R. J. Redmon, and D. Danskin (2015), Large-amplitude GPS TEC variations associated with Pc5–6 magnetic field variations observed on the ground and at geosynchronous orbit, *J. Geophys. Res. Space Physics*, *120*, 7798–7821, doi:10.1002/2015JA021517.